Biol. Cybern. 59, 303–312 (1988)

Biological Cybernetics

A Modular Analog Neuron-Model for Research and Teaching

U. T. Koch and M. Brunner

Fachbereich Biologie der Universität, Postfach 3049, D-6750 Kaiserslautern, Federal Republic of Germany

Abstract. An analog electronic neuron for modeling neuronal networks and for teaching purposes is presented. The circuitry represents a new approach, since ionic channels are all modeled by fast relay switches in combination with resistors. Thus, the synapse design includes nonlinear PSP superposition and reversal potentials. The spike is modeled with Na^+ and K^+ currents. Detailed circuit diagrams and examples of performance are given. Besides its use in network research, the model has been successfully used over 3 years of teaching practice.

1 Introduction

Analog neuron models (neuromimes) have been designed and built in a considerable variety by a great number of authors. An overview was given by Jenik (1962) and, more recently by MacGregor and Lewis (1977). Since then, only very few new designs of neuromines have appeared (Mitchell and Friesen 1981; Scott 1977), except for the purpose of school teaching (e.g. Basse-Lüsebrink and Lorenz 1984; Laug and Matzat 1980).

In terms of precision, the neuromime of Lewis (1968) performs to the highest expectation, but was too costly to be used in network simulations. The reduced version, also described in Lewis (1968) was quite successful since it led to several simulations of interesting small networks (Wilson and Waldron 1968; Friesen et al. 1976; Friesen and Stent 1977; Friesen and Wyman 1980).

This model was built using transistors and some other very nonlinear components, that were skilfully taylored to mimick many of the unique features of real neurons. To analyze and understand the circuitry of these neuromimes needs a thorough training in electronic circuit design, which can not always be expected from a neurophysiologist and even less from a biology student. A thorough understanding of the circuit, however, is essential if one wants to vary the properties of the neuromime to model different types of neurons. Later versions were built (French and Stein 1970; MacGregor and Oliver 1974; Eilts-Grim and Wiese 1984; Mitchell and Friesen 1981) using operational amplifiers and other integrated circuits which are easier to analyze and understand, yet they all lack one or the other features that are important in the performance of the model.

Considering the scope of possible applications in the research on of small networks and high level teaching, the following design goals seem to be of major importance:

1) to incorporate nonlinear superposition of postsynaptic potentials. This models saturation effects due to the limited equilibrium potentials, especially in inhibition (Tuckwell 1986);

2) to include the DC-coupled reset effects of the spike elicited K^+-conductance on the dendritic region;

3) to work out a satisfactory compromise between modelling accuracy and circuit simplicity;

4) to aim at a 1:1 correspondance between the functional role of each component in the model circuit and the equivalent element of the real neuron, in order to

a) achieve a high success rate in teaching
b) enable the user to modify the model to fit his data

5) to provide a modular design to permit construction of complicated single neurons or to incorporate special types of elements (modifiable synapses, nonspiking units, etc.)

In this work we intended to construct a neuron model fulfilling the above requirements. We have tried to use new circuitry that would be simple enough to be understandable, yet close enough to the principles of

neurophysiology to produce realistic performance at controlled costs, even if extended to networks of tens of neurons.

2 Elements of the Neuron Model

The neural modeling system consists of several subunits, modules, which are usually interconnected as illustrated in Fig. 1 to form a complete model neuron. The basic modules are: axonal membrane, synapse, dendritic membrane, and spike generator. In addition, there are three voltage sources labeled Na^+ ($+550$ mV)[1], K^+ (-750 mV)[1] and Cl^- (-650 mV)[1] to simulate the Nernst potentials generated by these ions, and a standard ± 15 V and $+5$ V power supply for driving the electronics. The connectors between modules carry these voltages to each point in the model.

2.1 Axonal Membrane

As in the real neuron, the resting potential is generated by an equilibrium of leakage currents, which are generated by the Nernst potentials of K^+ (-750 mV) and Na^+ ($+550$ mV) and the associated leakage pores, here modeled by resistors R_{Na} and R_K (Fig. 2a). Since R_K (500 KΩ) is much smaller than R_{Na} (3, 3 MΩ), the resting potential (-600 mV) is close to the potassium potential. A capacitor ($C_M = 0.01$ μF) mimicks the membrane capcitance of this elementary piece of membrane. The individual membrane units are interconnected by the longitudinal resistances R_L (20 kΩ), mimicking the resistance of the column of electrolyte enclosed by the axonal membrane. An array of four such unitary membraneous elements forms the "axonal membrane". Note that at each end of the passive chain, a longitudinal resistor of half the standard value permits the interconnection of axonal elements to form arbitrary lengths of "neuronal cable". The axonal membrane also carries a voltage follower amplifier the input of which can be connected to any point in the axon to give a low impedance output of the membrane potential.

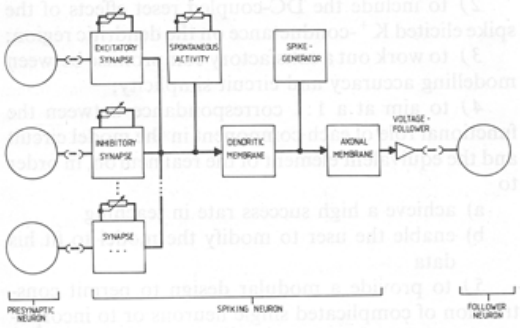

Fig. 1. Schematic diagram of a standard model neuron built from individual modules. Each module is a functional unit which can be connected to other modules to form more complex neurons

[1] For ease of handling, all voltages in the model have been set ten times higher than in reality

2.2 Chemical Synapse

The synapse (Fig. 2b) consists of a threshold detector (comparator) simulating the voltage sensitive Ca^{2+}-gates in the presynaptic terminal. Whenever and as long as the input voltage V_i is above a preset threshold (TP, usually -200 mV), a reed relay switch is activated, which simulates the ion channels of the postsynaptic membrane activated by the transmitter. For the duration of the input spike, the switch connects the inside of the postsynaptic neurone membrane to either the Na^+ (excitatory) or the K^+ (inhibitory) potential. The construction permits also the Cl^- potential to be used, but this option is omitted here for clarity. The amount of current flow is determined by the potential difference between the Na^+ (or K^+) potential and the postsynaptic membrane and a resistor R_S which mimicks the coupling strength of the synapse. R_S can either be an adjustable potentiometer, or a set of resistors selected with 3 rows of step switches. In this case, the setting of the step switches can be made to read directly in conductivity values (cf. Fig. 3b). It is clear that current flows only for the duration of the spike, thus the total input charge is dependent on spike width. The relay provides absolute separation of the presynaptic and postsynaptic potentials as in real chemical synapses.

2.3 Dendritic Membrane

The dendritic membrane (Fig. 2c) serves to receive and integrate the synaptic currents and to transmit them to the spike generating zone. In general, it has a structure similar to the axonal membrane, however its time constant ($R_{Na} \| R_K \cdot C_M$) is much longer. It is this time constant that governs the decay time of the postsynaptic potentials and therefore it lies in the range of 10 to 300 ms. In contrast to the axonal membrane, the dendritic membrane is asymmetric. At the synaptic side, it has a very small resistance, while there is a much higher resistance towards the spike generator. This simulates a certain length of the dendrite which seperates dendritic zones and spike generator. The dendritic membrane also contains a current source (represented by R_C in Fig. 2c) which can be set to mimic

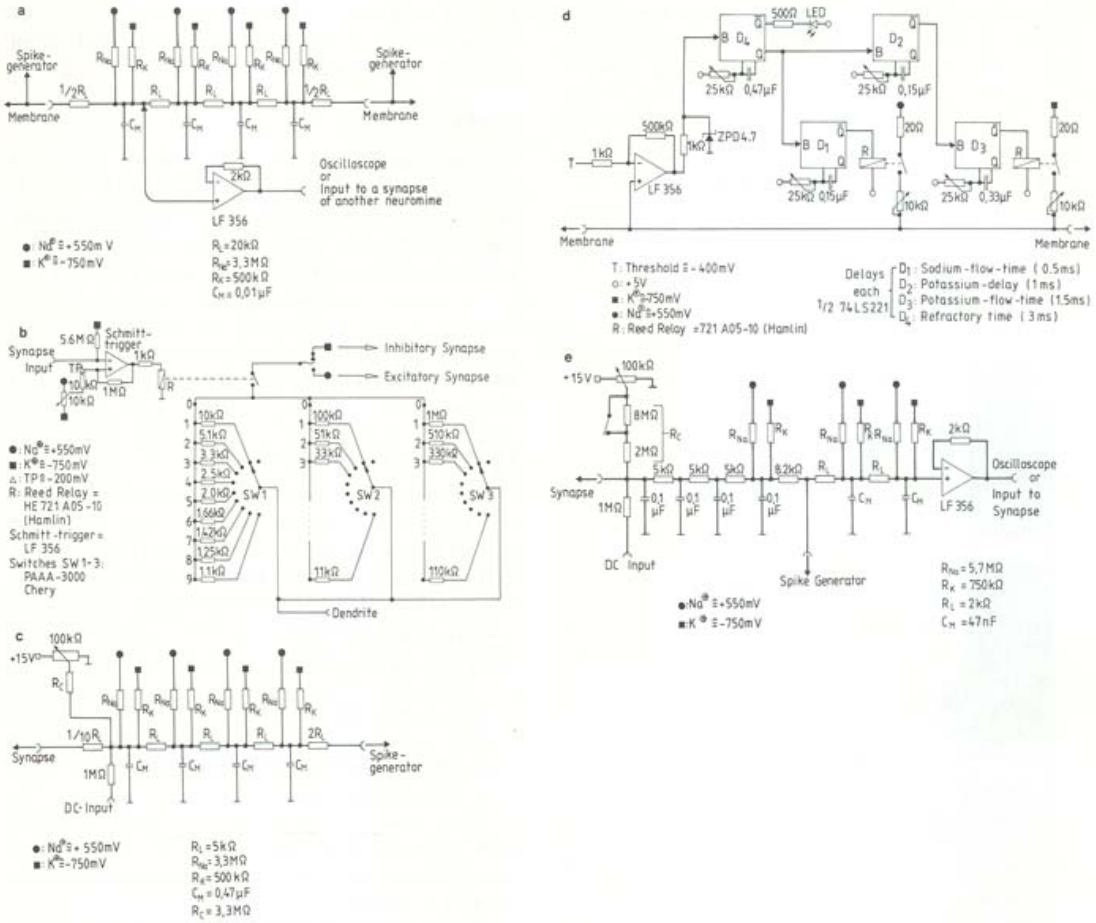

Fig. 2. a Circuit diagram of an axonal membrane module. The module consists of 4 subunits each modelling a patch of passive axonal membrane. Leakage resistors R_{Na} and R_K simulate sodium and potassium leakage pores. R_L is the longitudinal resistance of the intracellular fluid, C_M is the membrane capacitance. **b** Circuit diagram of a synaptic module. Via the Schmitt trigger, a spike at the input closes the contacts of the Reed relay R. The total amount of charge transferred to the dendrite depends on spike duration, cell potential and the setting of the switches $SW1$, $SW2$, $SW3$ which determine the resistance R_S. The "coupling factor" of the synapse is proportional to $1/R_S$. The resistance values are chosen such that the readings of the switches represent directly the coupling factor. In the student model, the switches and resistors are replaced by a single 100 kΩ potentiometer. **c** Circuit diagram of a dendritic module. The structure is almost identical to the axon module. The leakage resistors R_{Na}, R_K are the same as for the axonal module, while the longitudinal resistance is 4 times smaller. The membrane capacitance increased considerably to produce appropriate PSP decay time constants. **d** Circuit diagram of the spike generator module. An array of 4 monoflops $D_1 - D_4$ is triggered by a membrane potential that rises above threshold T. At first, the sodium channel is opened (duration D_1); then the potassium channel opens (D_3). D_4 controls absolute refractoryness. **e** Circuit diagram of the axo-dendritic module. This unit combines the functions of a dendrite and an axon for standard applications. The dendritic section (left) serves to accept and shape post-synaptic current pulses, while the axonal section (right) serves to shape the form of the spike produced by the spike generator

low level continous excitation necessary e.g. for spontaneous activity.

2.4 Spike Generator

In the design of the spike generator (Fig. 2d), it was not attempted to precisely simulate the Hodgkin-Huxley equations. Rather a very simplified directly activated sodium channel and a delayed potassium channel, each of fixed duration and conductance was used. The spike generator consists of two reed relay switches, one simulating sodium, the other potassium ion gates. They are controlled by a chain of 4 digital delay circuits (one-shots) $D_1 - D_4$. Whenever the membrane voltage

passes the threshold of −400 mV from below, the sodium relay is activated for about 0.5 ms (D_1). After a delay (D_2) of about 0.6 ms, the potassium relay is switched on and remains activated for about 1.5 ms (D_3). A further delay circuit (D_4) is used to block triggering of the delay chain during the absolute refractory time of 3 ms. The switching times and the conductance values of the Na^+ and K^+ channels can be finely adjusted, such that individual variability of the components is eliminated and a spike of standard form can be produced.

2.5 The Axo-Dendritic Unit

A more compact version of the passive membrane components exists in the axo-dendritic unit (Fig. 2e). It consists of a piece of dendritic membrane, the coupling resistor to the spike generator, and a small section of axonal membrane on which the spike generator can act. A voltage follower amplifier for the membrane potential output is provided as well. This unit is especially useful in the simulation of small neuronal networks, since it permits a more compact design of a neuron.

2.6 Physical Construction

The elements of the neuron model have been built in two versions. In the table version, each element is mounted on a PC board 140 × 50 mm (Fig. 3a). Each PC board (module) carries at one end a male and at the other end a female 13 pole connector. The modules can thus be easily connected to "chains", at the end of which the supply voltages are applied with a connector. Each chain then is one neuron. In the plug-in version, a spike generator, an axo-dendritic unit and four synapses are each mounted on small PC boards 80 × 40 mm which are plugged onto a "motherboard" of 100 × 140 mm (Fig. 3b).

Thus, each plug in-unit (50 mm wide × 130 mm high × 140 mm deep) contains a model neuron with 4 input synapses. Here, the synaptic coupling factors are set with step switches.

The advantage of the table version is high versatility for modeling special kinds of neurons or experimenting with the neuronal elements. The plug-in version is much more compact, and is easier to use in

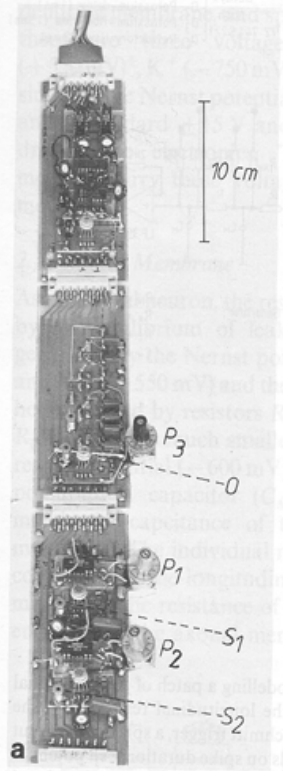

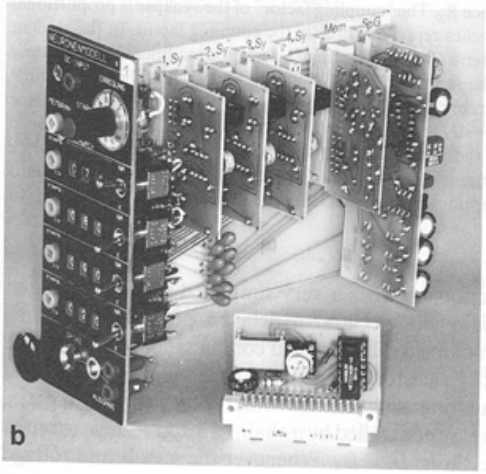

Fig. 3. a Photograph of the table version, as viewed obliquely from above. A complete model neuron consisting of a spike generator (top) an axodendritic unit (middle) and a double synapse (below) is shown. Inputs from other neurons are applied to ports S_1, S_2. The output (membrane potential + spikes) is found at plug O. This neuron was put together by students attending the neuromime course. The integrated circuits are mounted on dedicated mini PC boards which contain a lot of prewiring. They are mounted together with the other components on a larger carrier PC board that also serves to provide the voltages running through the system. The synaptic coupling factor is adjusted at P_1, P_2, wheras the spontaneous firing rate can be set at P_3. **b** Photograph of the plug-in version, containing (from right to left) spike generator, axodendritic membrane and 4 synapses. The front plate (50 × 160 mm) carries 4 sets of push button switches to adjust the synaptic coupling factors. The value appearing in the windows is directly proportional to PSP size

the simulation of small networks, because synaptic connections can be made more easily and the synaptic coupling factors can be set reproducibly and with high precision.

3 Results

3.1 Properties of the Neuronal Elements

3.1.1 Length Constant of the Axonal Membrane. The length constant was measured by connecting a chain of 6 model axonal elements together. At one end, an impulse of 1 ms width was applied, and the resulting decay of the signal amplitude was measured at each section point. The amplitude was plotted on a log scale versus the number of sections (Fig. 4). As in the cable theory, the expected exponential decay is observed, exept for the last few sections of the chain. The length constant was determined from this graph to be 5 sections.

3.1.2 Time Constant of the Dendritic and Axonal Membranes. The time constant of the dendritic membrane was determined using a synapse as pulsed current source. The synapse was triggered by short positive rectangular pulses of 1 ms width. One can see that the postsynaptic potential has a fast rise time and a slower exponential decay. In the circuit shown in Fig. 2c, a time constant of 225 ms was measured. This is basically determined by $(R_{Na} \| R_K \cdot C_M)$. By varying R_{Na} and R_K and/or C_M, one can achieve very short or very long PSP's. To be able to conduct spike impulses, the axonal membrane must have a sufficiently short time constant. We measured 4.4 ms. A time constant of this value would be not very useful in a dendritic membrane element. This is the main reason, why dendritic and axonal membranes must have different characteristics.

3.1.3 Spike Generator. The spike generator can be adjusted best if it is mounted into a complete model neuron, with a dc-setting sufficient for spontaneous spiking. A long open time and a high current intensity of the "sodium channel" generates a sharply onsetting spike with high amplitude. The open duration and current intensity of the "K^+-channel" control the steepness of the spike's decay and the amount of hyperpolarization which is also transmitted to the dendritic region resulting in a "reset" of the cell potential. The positive charges applied to the membrane by the Na^+-channel must be balanced by the negative charges flowing in from the K^+-channel. The balance must, infact, remain a little bit in favor of K^+, this maintains the stability of the neuron. On the other hand, this balance controls the current sensitivity of the neuron. If a positive current is applied to the membrane, the membrane potential will rise from the resting potential to the threshold, where one spike is fired. Due to the coupling resistor, there is a reset effect on the synaptic membrane potential. The smaller the reset effect, the shorter will be the time to drive the membrane to threshold again. Thus, a high K^+ overweight will generate a modest increase of spike frequency for an increase of excitatory Dc current. With a small K^+ overweight, the neuron responds to small stimulating currents with high spike rates (cf. Fig. 5).

3.1.4 Dependence of Synaptic Potential Parameters on Cell Potentials. During the activity of a synapse (closed time of reed relay = opening time of the post-

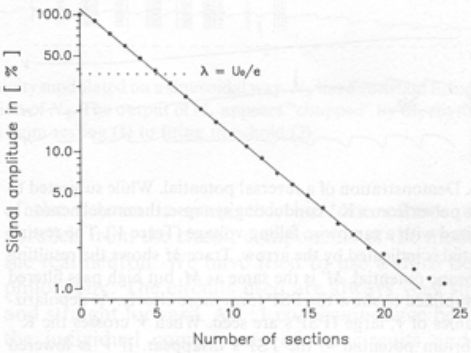

Fig. 4. Plot of the amplitude of a signal transmitted through a chain of 6 axonal modules versus the distance (measured in sections) from the signal origin. A strictly exponential decay, as predicted by cable theory, is observed. The length constant of our model axon is 5 sections (=1.25 modules)

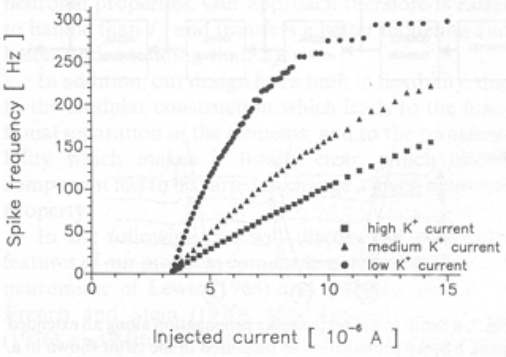

Fig. 5. Reaction of a model neurone to Dc current injection. The 3 curves have been generated by changing the conductivity of the K^+-channel in the spike generator to high (squares) medium (triangles) or low (dots) values. At low K^+ conductivity, there is only a small reset effect of the K^+-current on the neurone. Hence, the injected current needs a small time to recharge the membrane to threshold. This means a high spike rate per μA of injected current

synaptic ion gates), a short current pulse is generated. The current intensity I depends not only on the value of the synaptic coupling factor R_S, but also on the actual potential of the membrane. If the dendritic membrane is hyperpolarized to e.g. the potassium Nernst potential, then an IPSP due to a potassium current should disappear (reversal potential), which it does as shown in Fig. 6. If the membrane potential is lowered further, then the IPSPs will turn into EPSPs.

3.2 Results from Simulation Experiments

3.2.1 Signal Propagation in an Axon. In Fig. 7a, a setup of alternating spike generators and membrane sections is illustrated, built from elements of the table

Fig. 6. Demonstration of a reversal potential. While subjected to inputs pulses from a K^+ conducting synapse, the model neuron is polarized with a rampwise falling voltage (Trace *V*). The resting potential is indicated by the arrow. Trace *M* shows the resulting membrane potential, *M'* is the same as *M*, but high pass filtered and amplified to show the PSP form more clearly. At depolarizing values of *V*, large IPSP's are seen. When *V* crosses the K^+ equilibrium potential *, the PSP's disappear. If *V* is lowered further, the former IPSP's turn into EPSP's

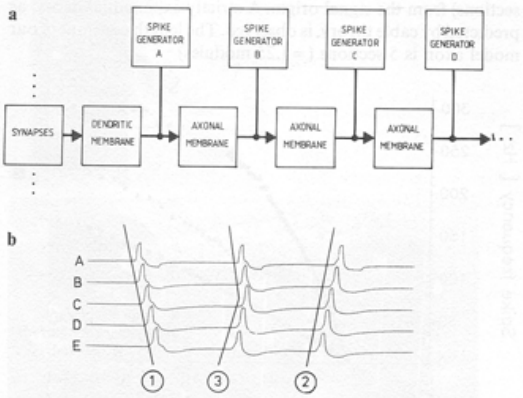

Fig. 7. a Setup to model the spike propagation along an extended axon. **b** Spike propagation as measured in the ciruit shown in **a**. Spike signals were measured at each membrane module. Event (1) shows orthodrome spike propagation. If a spike is started at the end of the neuron (spike generator *E*), antidrome conduction can be observed (2). In (3) a spike has been released simultaneously at *A* and *E*. Both spikes reach module *C* at the same time and propagation is stopped (occlusion). The straight lines were drawn into the recordings to emphasize the time shifts between the different channels

version. A spike as generated in a spike generator (*A*) propagates passively along the membrane element, until it reaches the next spike generator (*B*). When the passively attenuated signal crosses the threshold level of *B*, a new spike is generated in generator *B*. Its spike propagates passively both forwards towards generator *C*, and also backwards towards *A*. But in *A*, a spike cannot be elicited because of refractoriness. Thus, the propagating direction of a spike is maintained. As in the real neurone, the model axon has no principal preference of direction: spikes can propagate just as well in the other direction. This is demonstrated in Fig. 7b. Whenever two spikes start simultaneously at each end of the model axon, they meet in the middle. Then each spike runs into the refractory zone of the other, and conduction is terminated (occlusion).

3.2.2 Synaptic Computation. Fig. 8a shows a setup of three neurones, N_1, N_2, N_3. N_2 receives excitatory input from a slowly variable *AC* input (e.g. a "receptor potential") and is excitatory to N_1. N_3 is spontaneously active and has an inhibitory synapse with N_1. When N_2 is silent (Fig. 8b), the IPSP's from N_3 are small, since the resting potential of N_1 is close to the potassium potential. But when N_2 is active, the IPSP's become much larger and are capable of interrupting efficiently the steady exitation from N_2. Figure 8b thus shows an example of PSP size changes due to changes in the actual cell potential.

3.2.3 Ring Oscillator. An example of a simple neuronal oscillator (see e.g. Kling and Szèkely 1968) is shown in Fig. 9a. Three neurones are connected with inhibitory synapses in a circle. They also all receive constant exitation of equal size into their DC inputs. Figure 9b shows the oscillatory pattern for different values of DC exitation. Using the axo-dendritic unit, the longest period duration was 500 ms, the shortest was 25 ms. Thus a ratio of 1 : 20 between minimum and maximum period duration could be achieved.

3.2.4 Cricket Song Generator. This oscillator (Fig. 10a) is built to produce a spike pattern as recorded from e.g. the wing closer muscles of a cricket *(Gryllus campestris)* producing the calling song. Neuron N_1 has a constant DC input, which enables it to fire at a constant rate of 30 Hz. The synaptic coupling factors at the synapses S_2, S_3, and S_4 are set such that a single EPSP cannot elicit a spike. If a second EPSP arrives within 50 ms, a spike will be triggered. Thus, whenever N_1 begins to fire after an interuption N_2, N_3, and N_4 each omit the first spike of their precursor. N_4 very strongly activates the relay cell N_5, which in turn has a very strong inhibitory synapse to N_1. Each time N_4 fires a spike, a strong IPSP is generated in N_1 to

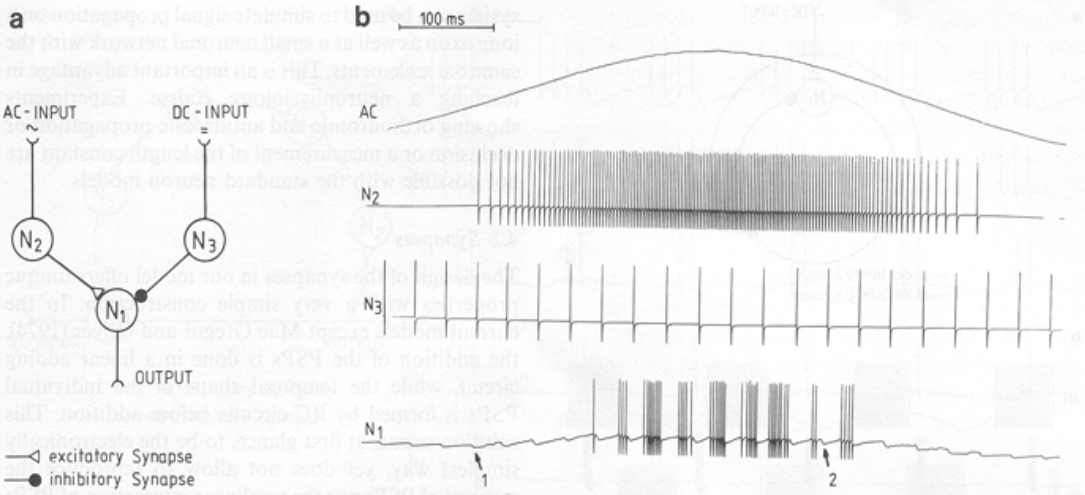

Fig. 8. a Small network of 3 neurons N_1 is exited by N_2 which has an activity modulated on a sinusoidal way. N_3 has a constant firing rate and inhibits N_1. **b** The exitatory influence of N_2 is gated by the inhibition of N_3. The output of N_1 appears "chopped" by the rhythm of N_3. Note that the size of the IPSP's grows as the cell potential rises from resting (1) to firing threshold (2)

interrupt the spontaneous spike series (Fig. 10b). In this way, packages of exactly 4 pulses of constant repetition rate are generated. If the synapses N_4-N_5 or N_5-N_1 are changed or if N_5 is inhibited to some degree, the pause between the chirps is reduced. If N_5 is inhibited completely, N_1 will run free. This corresponds to the "rivalry song". The correct setting of the coupling factor at S_2, S_3, S_4 was determined in the setup. It can vary between 48 and 70 units ($=14.2$ ...20. 8 kΩ).

3.3 Teaching Experiences

The table version has been used in advanced student courses in neurophysiology in the last 3 years. The students build one of each element of the system. They determine the individual properties of the elements and connect them to complete neuron models. Using the model with its modular structure, a very profound understanding of neuronal function can be achieved. The students show very strong interest and cooperation, especially in the last phases, where all units produced in the course are used to set up more complicated networks.

4 Discussion

In the design of an analog neuron model, two basic divergent pathways have been followed: *1)* an extensive, almost complete and exact simulation of the Hodgkin Huxley kinetics and the membrane properties. *2)* a "black box" approach, where the function of the neuron is simulated, but one cannot draw parallels from the circuit components of the model to the real neuron. We have tried to use a third design philosophy: The circuits used are always very simple and straight forward. A 1:1 correspondance between the individual components of the circuits and the properties of the real neuronal elements is always aimed at. In cases, where more complicated circuitry would be needed to give a precise simulation, we have designed first order approximative solutions, still maintaining the transferability of circuit properties to neuronal properties. Our approach therefore is easier to handle than *1)* and transfers a better modeling and better understanding than *2)*.

In addition, our design has a built in flexibility, due to the modular construction which leads to the functional separation of the elements, and to the transferability which makes it totally clear, which circuit component has to be varied to change a given neuronal property.

In the following, we will discuss the individual features of our model in comparison with the extensive neuromime of Lewis (1968) and with the models of French and Stein (1970), Mac Gregor and Oliver (1976), and Mitchell and Friesen (1984). The last three were selected because they are the most recent designs and use operational amplifiers instead of transistors.

4.1 Modularity

To our knowledge, only the extensive model of Lewis (1968) permitted a similar variety of experiments. Our

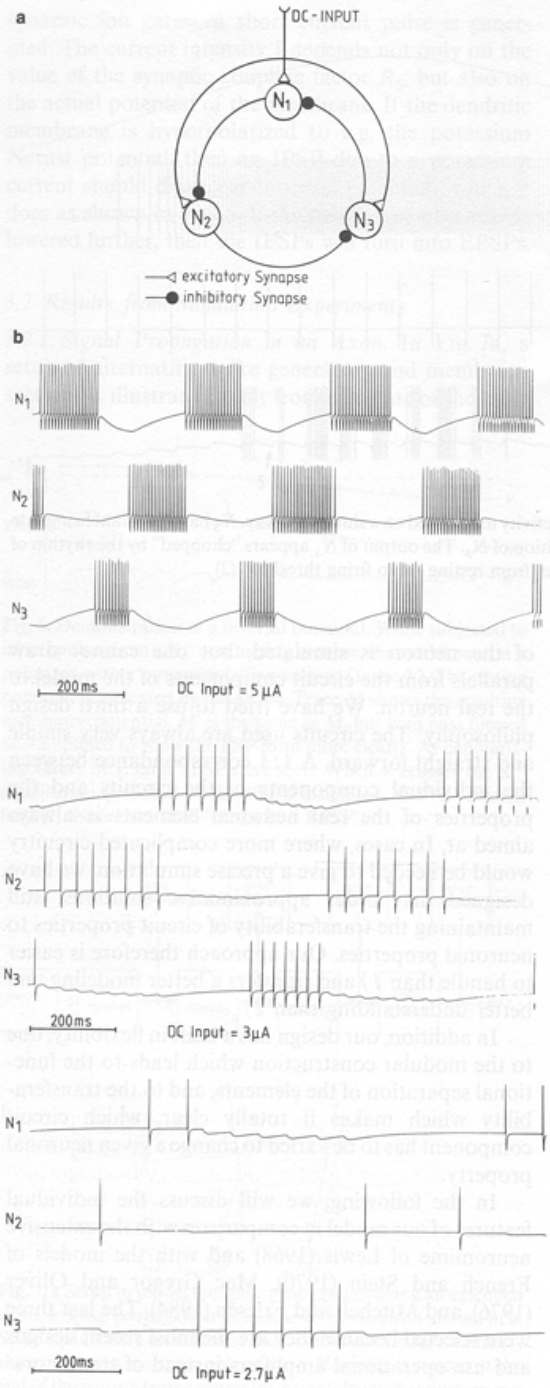

Fig. 9. **a** Three-neuron circuit providing oscillation by cyclic inhibition. **b** Output patterns of the oscillator shown in **a**. The three different patterns result from different Dc-exitation of the neurons. As shown, a large dynamic range of oscillation frequencies can be achieved

system can be used to simulate signal propagation on a long axon as well as a small neuronal network with the same basic elements. This is an important advantage in teaching a neurophysiology course. Experiments showing orthodromic and antidromic propagation or occlusion or a measurement of the length constant are not possible with the standard neuron models.

4.2 Synapses

The design of the synapses in our model offers unique properties with a very simple construction. In the current models except Mac Gregor and Oliver (1974), the addition of the PSPs is done in a linear adding circuit, while the temporal shape of the individual PSPs is formed by RC-circuits before addition. This solution seems, at first glance, to be the electronically simplest way, yet does not allow to reproduce the reversal of PSPs nor the nonlinear interaction of PSPs as found in real neurons. Tuckwell (1986) has shown that these nonlinearities may produce special effects that may not be neglected in many cases. Furthermore, there is an effect of total synaptic conductivity on the time constants of the PSP decays: a high conductivity, e.g. as produced by large excitatory and simultaneous inhibitory activity contributes to shorten the PSP decay times; this effect is automatically included in our model. In the plug-in version, we have introduced a scheme to set the synaptic coupling factors in a reproducible way, a feature which is a great advantage in setting up neuronal networks reproducibly and in testing the stability of a network against variation in synaptic coupling factors. The readings of the digital switches are linear in conductivity, this means that the readings are linearly correlated to PSP size within the linear range of the synapse. These features have proved to be essential in working with more sophisticated small networks (Bässler, personal communication).

Finally, our synapse design permits the influence of spike width on PSP size. This feature permits to model changes in synaptic transmission by spike broadening as demonstrated by Klein et al. (1980) in *Aplysia*, as well as other presynaptic modulation effects.

4.3 Spike Generator

Although our spike generator is very simple, it permits to model some of the important blocking experiments routinely used in the analysis of neuronal function. Thus, the effects of TTX can be modeled by disabling the Na^+ delay unit, and likewise, an application of TEA can be simulated by disabling the K^+ delay unit. The direct connection between the spike generator and the dendritic unit permits a further realistic feature: each action potential produces a reset effect on the synaptic region mediated by the strong hyperpolariz-

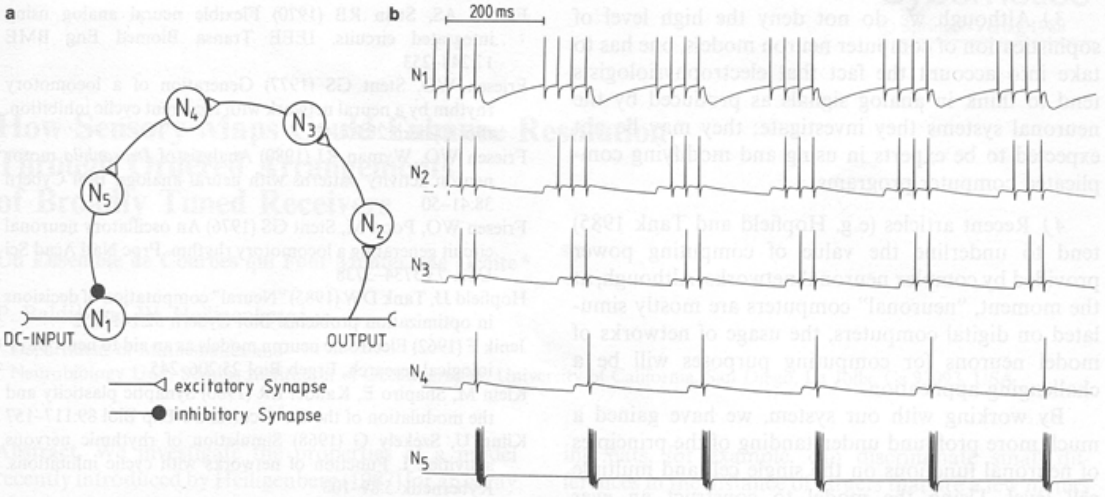

Fig. 10. a Oscillatory circuit generating a spike pattern as observed in a cricket producing the calling song. The excitatory synapses N_1-N_2, N_2-N_3, and N_3-N_4 are adjusted such that a single EPSP cannot trigger a spike, but if a second EPSP arrives within 50 ms, a spike will be activated. N_4-N_5 is a rather strong exitatory, N_5-N_1 a strong inhibitory synapse. **b** Output patterns of the circuit shown in **a**. N_2, N_3, N_4 each start firing after the arrival of the second EPSP. The spike in N_4 releases a large burst of spikes in N_5. This burst causes strong inhibition in N_1 and thus generates a long pause in N_1. The pause and the frequency within the burst can be adjusted independently, a feature also found in the real cricket's pattern generator

ation due to the late K^+ currents. A similar feedback pathway in Mitchell & Friesen models does not serve the same purpose, since it is AC-coupled. The charge removal by the spike also helps in generating a realistic "spontaneous activity" without the need for a specific pacemaker potential. It works just like a depolarizing intracellular electrode.

4.4 Neuronal Circuits

The model of the inhibitory ring oscillator shows a very high dynamic range. Simply by varying the DC excitatory input, the frequency of the ring oscillator can be varied in a range of 20:1. This compares well to the range of 5:1 as demonstrated with the (Lewis *b*) model by Friesen and Stent (1977)). The cricket song generator can be regarded as an example of innovative neuronal circuit design using the features of our system. It contains the most important properties of the real crickets' song pattern generator: the syllable rhythm is very stable and unaffected by variations of the chirp rate (cf. Weber 1974). In addition, the transition to the rivalry song can be simulated by inhibition of a single neuron (N_5) in the circuit.

4.5 Other Aspects

In the teaching environment, the design of our model is very helpful because it contains all elements of the standard equivalent circuits used to explain the functioning of neurons and very few other elements that need explaining. Ionic gates are represented as switches, which comes very close to their real function. In the design presented here, several features such as accomodation or post inhibitory rebound, have not been included. We are currently working on circuits to model these features in a way permitting a close resemblance with the molecular mechanisms behind these properties. We are also aware of the possibilities to replace the relay switches by solid state analog switches, which, however, are more susceptible to breakdown by unintentional electric pulses. We are also investigating the possibilities of simulating synapses between non-spiking neurons and other neurons, while retaining the basic character of our synapse design.

In the age of digital computers, one may raise the question if an analog electronic neuron model is not totally obsolete. Yet, there are several principal advantages of analog modeling:

1) The analog system always works in real time, regardless of the complexity of the neuronal network that can be constructed from our units. Interesting potential recordings can be simultaneously made from any point in the model.

2) The parameters controlling the behavior of a model network (such as the synaptic coupling constants) can be *directly* controlled by the experimenter, and the reaction of the system to these changes can be directly viewed in real time.

3) Although we do not deny the high level of sophistication of computer neuron models, one has to take into account the fact that electrophysiologists tend to think in analog signals as produced by the neuronal systems they investigate; they may be not expected to be experts in using and modifying complicated computer programs.

4) Recent articles (e.g. Hopfield and Tank 1985) tend to underline the value of computing power provided by complex neuronal networks. Although, at the moment, "neuronal" computers are mostly simulated on digital computers, the usage of networks of model neurons for computing purposes will be a challenging application.

By working with our system, we have gained a much more profound understanding of the principles of neuronal functions on the single cell and multiple cell level. Using the model to construct an ever increasing variety of neuronal networks results in a growing intuitive capability to understand the dynamics of neuronal networks and the rules of their design, which often turn out to be so different from our understanding trained in linearly interacting systems. This may be one of the reasons why our model has elicited such strong interest among fellow neurophysiologists.

Acknowledgements. We gratefully acknowledge the help of Mrs. S. Watt in typing the manuscript and of Mrs. I. Winkler-Reske in preparing the figures. We thank Roland Milli and Winfried Galm who helped decisively in different stages of the realization of the model. We are also grateful for intensive discussions with J. J. de Kramer (BASF). This work would not have been possible without the continuous support by Prof. U. Bässler. His increasing demands for flexibility and handling ease stimulated the further evolution of the design, and his comments were a vital feedback to ensure adequate design and function of our model.

References

Basse-Lüsebrink B, Lorenz R (1984) Bau und Betrieb eines elektronischen Nervenfunktionsmodelles. Prax Naturwiss 5:135–140

Eilts-Grimm K, Wiese K (1984) An electrical analogue model for frequency dependent lateral inhibition refering to the omega neurons in the auditory pathway of the cricket. Biol Cybern 51:45–52

French AS, Stein RB (1970) Flexible neural analog using integrated circuits. IEEE Transa Biomed Eng BME 17:248–253

Friesen WO, Stent GS (1977) Generation of a locomotory rhythm by a neural network with recurrent cyclic inhibition. Biol Cybern 28:27–40

Friesen WO, Wyman RJ (1980) Analysis of *Drosophila* motor neuron activity patterns with neural analogs. Biol Cybern 38:41–50

Friesen WO, Poon M, Stent GS (1976) An oscillatory neuronal circuit generating a locomotory rhythm. Proc Natl Acad Sci USA 73:3734–3738

Hopfield JJ, Tank DW (1985) "Neural" computation of decisions in optimization problems. Biol Cybern 52:141–152

Jenik F (1962) Electronic neuron models as an aid to neurophysiological research. Ergeb Biol 25:206–245

Klein M, Shapiro E, Kandel ER (1980) Synaptic plasticity and the modulation of the Ca^{2+} current. J Exp Biol 89:117–157

Kling U, Székely G (1968) Simulation of rhythmic nervous activities. I. Function of networks with cyclic inhibitions. Kybernetik 5:89–103

Laug A, Matzat K (1980) Der Einsatz eines elektronischen Neuronenmodells im Unterricht. Biologieunterricht 16: 77–96

Lewis ER (1968) Using electronic circuits to model simple neuroelectric interactions. Proc IEEE 56:931–949

MacGregor RJ, Lewis ER (1977) Neural coding: models of electrical signal processing. In: Neural modeling. Plenum Press, New York London, pp 193–224

MacGregor RJ, Oliver RM (1974) A model for repetitive firing in neurons. Kybernetik 16:53–64

Mitchell CE, Friesen WO (1981) A neuromime system for neural circuit analysis. Biol Cybern 40:127–137

Scott PD (1977) A simple hardware model neurone. Proc Physiol Soc 269:19–20

Tuckwell HC (1986) On shunting inhibition. Biol Cybern 55:83–90

Weber T (1974) Elektrophysiologische Untersuchungen zur Entwicklung und zum Verlauf von Verhaltensweisen bei *Gryllus campestris* L. Dissertation, Universität Köln

Wilson DM, Waldron I (1968) Models for the generation of the motor output pattern in flying locusts. Proc IEEE 56:1058–1064

Received: February 18, 1988

Dr. U. T. Koch
Fachbereich Biologie der Universität
Postfach 3049
D-6750 Kaiserslautern
Federal Republic of Germany